Deep Instance Segmentation of Teeth in Panoramic X-Ray Images

6 authors, including:

Gil Jader
Universidade Federal da Bahia
2 PUBLICATIONS   **196** CITATIONS

Marco Ruiz
Universidade Federal da Bahia
4 PUBLICATIONS   **127** CITATIONS

Kalyf Abdalla Buzar Lima
Instituto Federal de Educação, Ciência e Tecnologia da Bahia (IFBA)
9 PUBLICATIONS   **183** CITATIONS

Luciano Oliveira
Universidade Federal da Bahia
72 PUBLICATIONS   **798** CITATIONS

Some of the authors of this publication are also working on these related projects:

Project Semantic pedestrian detection View project

Project Deep Instance Segmentation of Teeth in Panoramic X-Ray Images View project

Deep instance segmentation of teeth in panoramic X-ray images

Gil Jader*, Jefferson Fontinele*, Marco Ruiz*, Kalyf Abdalla *, Matheus Pithon [†], Luciano Oliveira*

* Intelligent Vision Research Lab
Federal University of Bahia
Email: see http://ivisionlab/members.html
[†] Southeast State University of Bahia
Email: matheuspithon@uesc.br

Abstract—In dentistry, radiological examinations help specialists by showing structure of the tooth bones with the goal of screening embedded teeth, bone abnormalities, cysts, tumors, infections, fractures, problems in the temporomandibular regions, just to cite a few. Sometimes, relying solely in the specialist's opinion can bring differences in the diagnoses, which can ultimately hinder the treatment. Although tools for complete automatic diagnosis are no yet expected, image pattern recognition has evolved towards decision support, mainly starting with the detection of teeth and their components in X-ray images. Tooth detection has been object of research during at least the last two decades, mainly relying in threshold and region-based methods. Following a different direction, this paper proposes to explore a deep learning method for instance segmentation of the teeth. To the best of our knowledge, it is the first system that detects and segment each tooth in panoramic X-ray images. It is noteworthy that this image type is the most challenging one to isolate teeth, since it shows other parts of patient's body (*e.g.*, chin, spine and jaws). We propose a segmentation system based on mask region-based convolutional neural network to accomplish an instance segmentation. Performance was thoroughly assessed from a 1500 challenging image data set, with high variation and containing 10 categories of different types of buccal image. By training the proposed system with only 193 images of mouth containing 32 teeth in average, using transfer learning strategies, we achieved 98% of accuracy, 88% of F1-score, 94% of precision, 84% of recall and 99% of specificity over 1224 unseen images, results very superior than other 10 unsupervised methods.

I. Introduction

From images obtained by X-rays, dentists can analyze the entire dental structure, planning (if necessary) patient's treatment. Indeed X-ray images are a tool that is used in dental medicine to check the state of the teeth, gums, jaws and bone structure of a mouth, allowing diagnosis of buccal problems. In dentistry, X-rays are divided into two categories: **Intraoral**, a radiographic technique performed with the film positioned in the buccal cavity (the X-ray image is obtained inside the mouth), and **extraoral**, in which the patient is positioned between the radiographic film and the X-ray source (the X-ray image is obtained outside the patient's mouth). In these two categories, there are three types of dental X-rays that are used most often in dental examinations: Extraoral panoramic radiography - also called **panoramic X-ray** or orthopanto-mography; intraoral bitewing radiography - or **bitewing X-ray**; and periapical intraoral radiography or only **periapical X-**
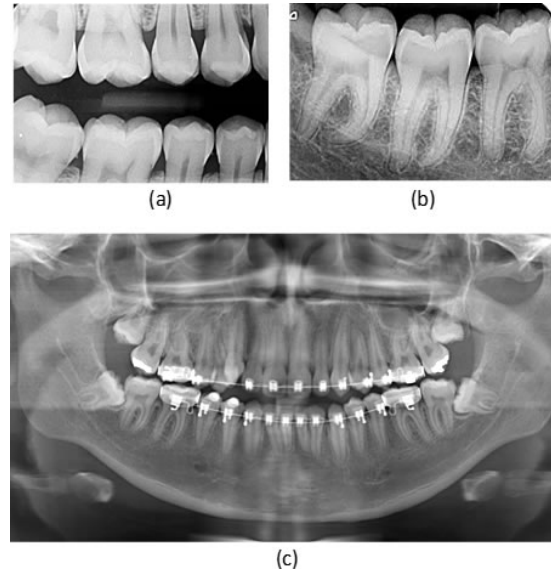

Fig. 1. Types of X-ray images: (a) Bitewing X-ray; (b) Periapical X-ray; (c) Panoramic X-ray.

rays. Figure 1 illustrates examples of these X-ray image types. Particularly, panoramic X-ray is a useful exam to complement the clinical examination in the diagnosis of dental diseases (caries or endodontic diseases). This type of examination allows the visualization of dental and buccal irregularities, such as: Teeth included, bone abnormalities, cysts, tumors, cancers, infections, post-accident fractures, temporomandibular joint disorders that cause pain in the ear, face, neck and head region. Commonly, dentists request panoramic view of the mouth as a preoperative examination of the teeth, and bone surgeries of the temporomandibular region [1], [2].

A. Training Mask R-CNN

Panoramic radiographs are not restricted to only an isolated part of the teeth, as occurs in intraoral radiographic images, also showing joints between the jaws and the skull, chin, spine and other details originated from the bones of the nasal and face areas. Other informations on panoramic radiographs make their images difficult to be analyzed, such as variations

TABLE I

CATEGORIZATION OF THE DATA SET IMAGES AND AVERAGE NUMBER OF TEETH PER CATEGORY.

| Number	Category	Images	Average number of teeth
1	Images with **all the teeth**, containing teeth with restoration and with dental appliance	73	32
2	Images with **all the teeth**, containing teeth with restoration and without dental appliance	220	32
3	Images with **all the teeth**, containing teeth without restoration and with dental appliance	45	32
4	Images with **all the teeth**, containing teeth without restoration and without dental appliance	140	32
5	Images containing dental implant	120	18
6	Images containing more than 32 teeth	170	37
7	Images **missing teeth**, containing teeth with restoration and dental appliance	115	27
8	Images **missing teeth**, containing teeth with restoration and without dental appliance	457	29
9	Images **missing teeth**, containing teeth without restoration and with dental appliance	45	28
10	Images **missing teeth**, containing teeth without restoration and without dental appliance	115	28
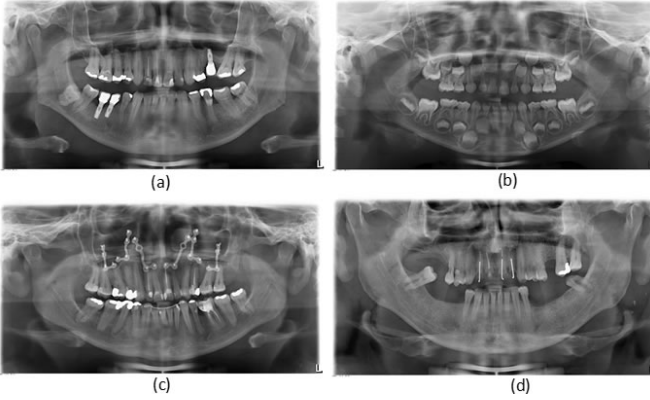
Fig. 2. Examples of some problems detected in panoramic X-ray images: (a) Dental implant, restored teeth, apex of some teeth; (b) supernumerary teeth; (c) devices for mandibular trauma; (d) missing and broken teeth.

of patient-to-patient teeth, artifacts used for restorations and prostheses, homogeneity in regions close to the objects of interest, space existing by a missing tooth, and limitation of acquisition methods. Figure 2 depicts some examples of these cases. In a nutshell, analysis of panoramic X-ray images depends on a careful work of the professional, who does not have automatic tools in his/her aid. This way, an automatic segmentation method to isolate parts of panoramic X-ray images could be a beginning of helping dentists in their diagnoses.

B. Related works

Unsupervised segmentation of teeth in X-ray images: So far, the vast majority of research in dental imaging relies on unsupervised pixel-wise segmentation [3]. Among these works, methods run over **bitewing images** [2], [4-15], **periapical** [16-29], or **panoramic** [1], [30-37]. According [3], 80% of the works studied use intra-oral images, such as bitewing or periapical, to perform their experiments. Some of these use more than one type of image in their experiments: Bitewing and periapical [38]; bitewing and panoramic [39]; periapical and panoramic [40]; bitewing, periapical and panoramic [41]. Most of the papers work with small data sets, usually ranging from 1 to 100 images [1], [4-5], [8-9], [12], [14-17], [19-20], [22-24], [26-30], [32-34], [37], [39]. [38] is the only one that used the largest number of images among the works reviewed in [3] (630 intraoral images). All works evaluated the performance of their proposed works, considering few variations in the data set.

Teeth segmentation in panoramic images: To the best of our knowledge, our work is the first one to exploit instance segmentation based on deep learning on panoramic X-ray images. The rest of the works follow an unsupported way for segmentation, such as: **Cluster-based** [30], **threshold-based** [1], [32-34], **region-based** [31], **boundary-based** [35-37].

Segmentation of other types of medical images: In [42], the authors trained an end-to-end convolutional network in order to segment neuronal structures in electronic microscopic cells. In [43], the authors proposed a spatially constrained convolutional neural Network (SC-CNN) to perform detection and classification of nuclei in histological images of routine colon cancer. A work with a detection system of lung cancer from a segmentation of images by pulmonary CT using a so-called U-net convolutional network is proposed in [44]. An organ segmentation method as a crucial step to obtain efficient computer-aided detection from chest radiography is proposed in [45]; the authors proposed a structure adversion corrective network (SCAN) to segment lung fields and heart image boundary.
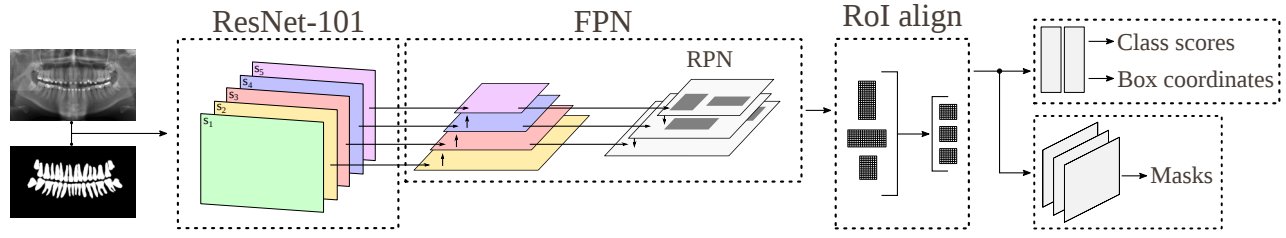
Fig. 3. Training process of the segmentation system. From left to right: X-ray images and annotation masks as inputs, ResNet101 backbone with 5-stage feature extractor (from S_1 to S_5), where the output of each ResNet stage, but S_1, forms a layer in the feature pyramid network (FPN); anchors are determined over FPN, and regions of interest (RoI) are computed (defining the region proposal network (RPN)) and, finally, aligned (RoI aligned). Outputs are the class scores and box coordinates, given by full connected network, and masks, given by a fully convolutional network.

C. Contributions

So far, most of works tackled the problem of tooth segmentation by using bitewing or periapical images, due to the difficulties to treat panoramic views of the buccal cavity. Bitewing and periapical images bring the view of the teeth more clearly and with less interferences of other bone structures. Data sets used in the works presents limitation to evaluate comprehensive applications of the proposed methods, bringing few images with small variations, even in the few works that exploited panoramic images.

To the best of our knowledge, this is the first work to rely explicitly in deep learning for instance segmentation on panoramic X-ray images of teeth. Therefore our work here could be considered seminal, even taking into account the way that it was evaluated: Based on our data set presented in [3], we used the 1500 panoramic images, with high variability and categorized in 10 different classes summarized in Table I, to train a deep network based on mask region-based convolutional neural network (Mask R-CNN). Results showed the powerful characteristic of the proposed system: Trained with just 193 buccal images, considering yet a transfer learning from MSCOCO data set [46], the system was capable to achieve 98% of accuracy, 88% of F1-score, 94% of precision, 84% of recall and, finally, 99% of specificity over 1224 images of mouths. These results were found by separating teeth in the training images (originally considering the dental structure as a whole in [3]), and exploiting the noise factor of the deep network with the separated teeth regards the original annotation. In words, the strategy of augmenting the number of the objects of interest (teeth instead of mouths) favored the system to reach high orders of magnitude in all performance metrics, and to be very superior than unsupervised methods evaluated in [3].

II. INSTANCE SEGMENTATION OF TEETH IN X-RAY IMAGES

The task of object detection aims at localizing and classifying individual objects. The goal of semantic segmentation is to classify each pixel of an object into known categories, without differentiating object instances. Instance segmentation combines these two classical computer vision tasks (detection and semantic segmentation), where each detected object is classified, localized and segmented. Our proposed system here use Mask R-CNN [47] for instance segmentation of teeth in X-ray images.

A. Deep network architecture details

Mask R-CNN architecture is depicted in Fig. 3. As an extension of the Faster R-CNN [48], Mask R-CNN includes a branch of convolutional networks to accomplish the instance segmentation task. After extracting features from ResNet101, these features compose a feature pyramid network (FPN), where ultimately anchors are defined and regions of interest (RoIs) are extracted. These two stages (FPN + anchors) form the region proposal network (RPN) introduced by [48]. After that, RoIs are aligned to have the same size. At the end, each fixed-size feature is: i) Classified as tooth or background (class scores); ii) localized by regressing the bounding box coordinates; and iii) per-pixel segmented by the fully convolutional network (FCN) [49] in each detected tooth bounding box (masks).

On our data set, only 193 buccal images were annotated. This amount of annotations was not sufficient to train Mask R-CNN from scratch due to the number of free parameters in the deep learning network. To cope with the lack of annotated data, pre-trained weights were taken from MSCOCO data set [46], which has 80 annotated objects for instance segmentation task. We only used the pre-trained weights in the backbone (ResNet 101) of the Mask-RCNN network. Just the weights of the top layers (RPN and so forth) were initialized with our data set.

The hyperparameters of the Mask training (*e.g.,* learning rate, number of epochs) were defined empirically by observing the training on a experiment with validation data. In this step, we split 193 annotated images into two distinct sets to train the segmentation network, to validate the results and to tune the hyperparameters. The tuned hyperparameters were used on the training step, whose results are described on Section III.

The training stage on our data set was performed on two-fold steps. On the first step, an Adam optimizer [50] was used with $\alpha = 10^{-3}$, $\beta_1 = 0.9$, $\beta_2 = 0.999$, and $\epsilon = 10^{-8}$. The weights of the head layers were training with 100 epochs. Adam optimizer was used to obtain a quick result of adjusting the weights for the new segmentation task. In the second step, a stochastic gradient-descent (SGD) optimizer was used,

Category	Accuracy	Specificity	Precision	Recall	F1-score
#1 (73)	0.98	0.99	0.92	0.91	0.92
#2 (60)	0.98	0.99	0.94	0.91	0.92
#3 (2)	0.97	0.99	0.96	0.77	0.85
#4 (67)	0.98	0.99	0.96	0.89	0.93
#5 (120)	0.98	0.99	0.94	0.82	0.87
#6 (170)	0.97	0.99	0.94	0.83	0.88
#7 (115)	0.97	0.98	0.80	0.90	0.84
#8 (457)	0.97	0.99	0.97	0.80	0.87
#9 (45)	0.98	0.99	0.96	0.88	0.92
#10 (115)	0.99	0.99	0.93	0.89	0.91
Weighted sum:	1195.83	1215.73	1146.63	1032.57	1082.11
Average±STD:	**0.98 ±0.008**	**0.99±0.006**	**0.94±0.06**	**0.84±0.07**	**0.88±0.05**
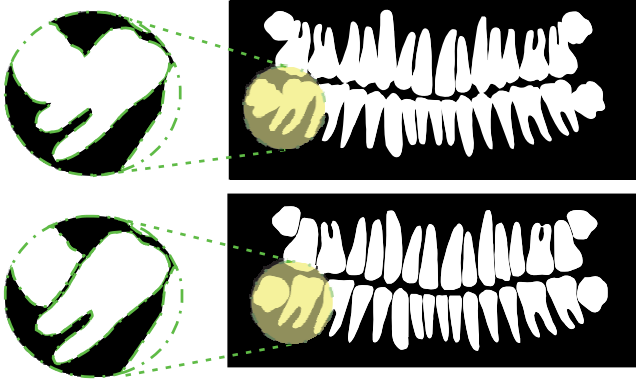
Fig. 4. Process of separating the teeth in the data set proposed by [3]. Zoomed tooth in the top is as it was in [3], and in the bottom is as it was changed here.

without any definition of momentum, with learning rate of 10^{-6}, to perform the fine tuning of the weights. In this last step, the weights of stages 4 and 5 from ResNet 101 (see Fig. 3), as well as the layers of the head, were considered to be trained. Each stage of ResNet 101 corresponds to a set of sequential convolutional layers with the same feature map size. The training was performed with an error rate of 10^6. The network weights resulting from this training stage were used in the evaluation and result comparison against other methods.

III. EXPERIMENTAL ANALYSIS

The annotation of 276 images in the first four categories (1, 2, 3 and 4) of the original data set [3] was modified by separating the teeth according to Fig. 4. Those categories were chosen since they present images with 32 teeth, located more or less in expected positions; 193 images were used for training (6987 teeth), while 83 images (3040 teeth) were used as a validation set to fine-tuning the deep network.

The process of splitting the teeth in each image was done so in order to train the Mask R-CNN with more samples (now, objects are the teeth, rather than an entire dental arch) than the originally gathered data set. This strategy demonstrated to be effective, even considering that 1224 test images was used as

the data set with entire dental arch annotation. After training the Mask R-CNN with 6987 tooth images (from 193 images), and fine-tuning the network parameters with the 3040 tooth images (from 83 images), 1224 dental arch images were used to evaluate the Mask R-CNN (by using original annotation of the mouth).

A. Quantitative analysis

To assess the performance of the segmenter, the following metrics were used: **accuracy** = $\frac{(TP+TN)}{(TP+FN+FP+TN)}$, **specificity** = $\frac{TN}{(TN+FP)}$, **precision** = $\frac{TP}{(TP+FP)}$, **recall** = $\frac{TP}{(TP+FN)}$, and **F1-score** = $\frac{2*Recall*Precision}{(Recall+Precision)}$, where TP, TN, FN and FP stand for true positive, true negative, false negative and false positive, respectively. These metrics were used in a pixel-wise fashion.

Following the methodology proposed by [3], a weighted average was computed considering the number of images for each category (weights), and the summation of the resulting metric for each image, all divided by the number of testing images. Table II summarizes the quantitative results found by our system. All standard deviations was found very low, indicating that all the individual results were all near the mean. This fact demonstrates that, although the data set was challenging, the proposed system achieves a good generalization and consistency in the results.

In a nutshell, results indicated a good balance between true negative/false negative (specificity, accuracy) and true positive/false positive (accuracy, precision and recall) rates, which are ultimately attested with the F1-score, computing the harmonic mean between recall and precision.

Mask R-CNN demonstrated highly superior results in comparison to unsupervised methods evaluated in [3]. Table III presents the results of the MASK R-CNN compared with the results of the unsupervised segmentation methods that were evaluated in [3]. Although the number of the testing images differs between the two classes of methods, the difference is not so high in order to hinder the comparison (1500 against 1224). In Table III, the best results of the unsupervised are highlighted as well as the results of MASK R-CNN. Except in **specificity**, whose result of the deep learning method was close
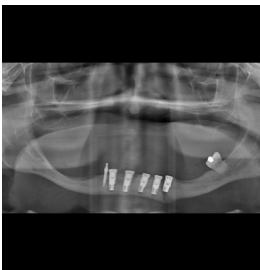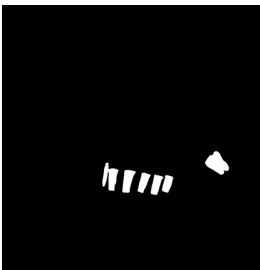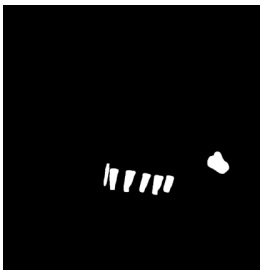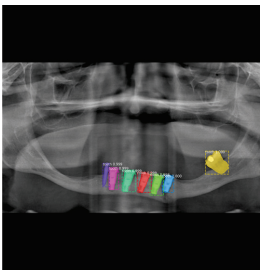
Fig. 5. Examples of best individual results, considering each metric. Most left column: metric type and value.
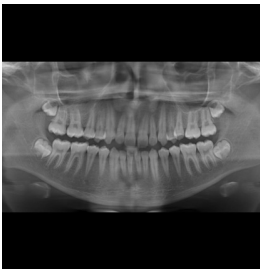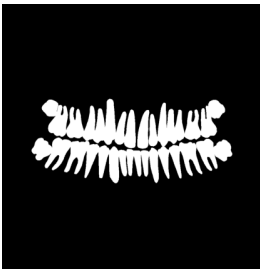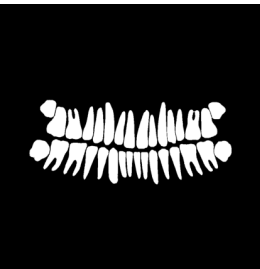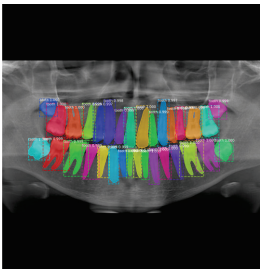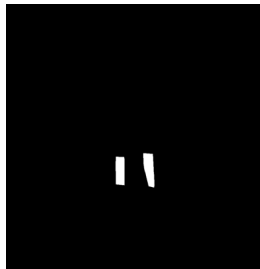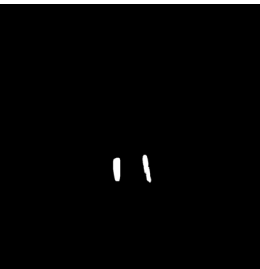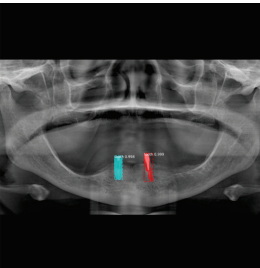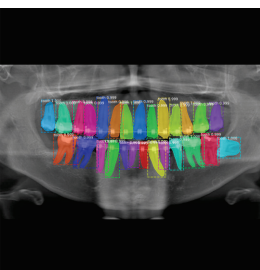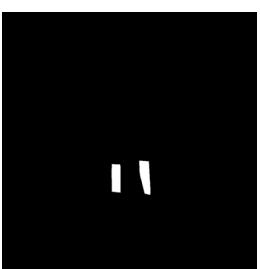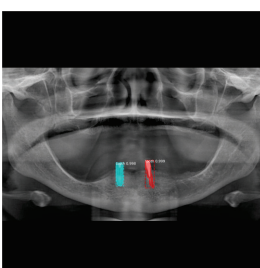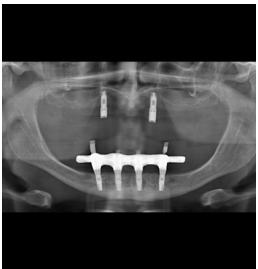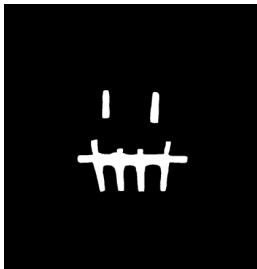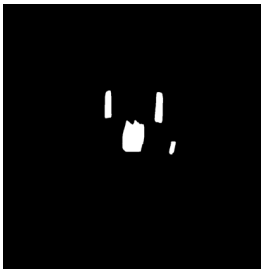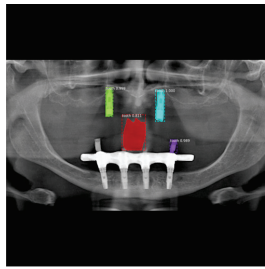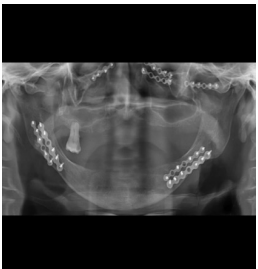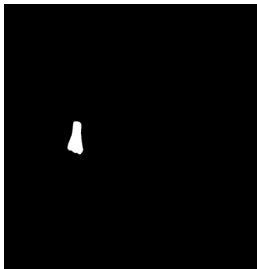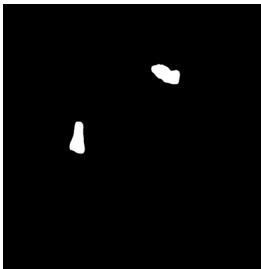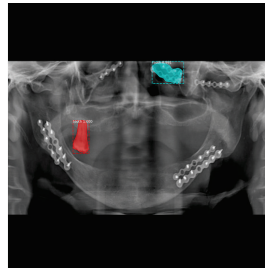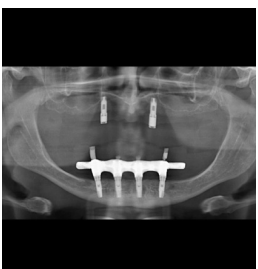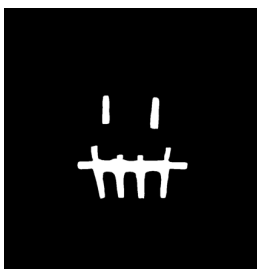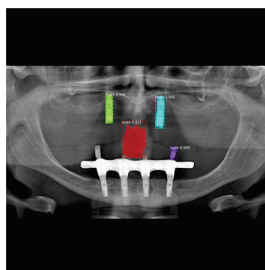
	Original	Groundtruth	Segmentation	Instance segmentation
Accuracy0.91				
F1-score0.29				
Precision0.48				
Recall0.17				
Specificity0.96				

Fig. 6. Examples of worst individual performance, considering each metric. Most left column: metric type and value.
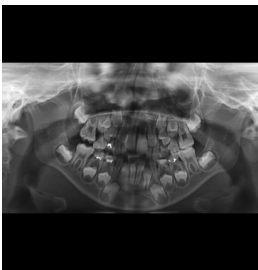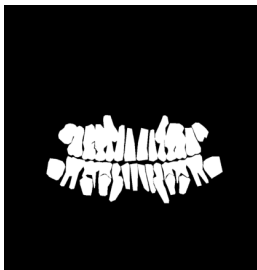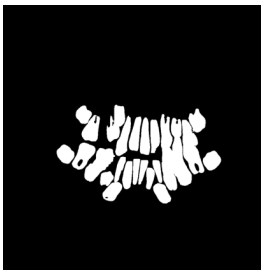
TABLE III
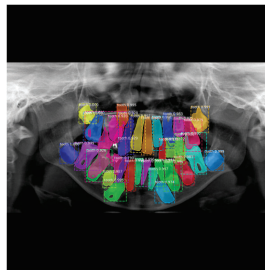COMPARISON OF THE UNSUPERVISED METHODS STUDIED IN [3] AND MASK R-CNN.

Method	Accuracy	Specificity	Precision	Recall	F1-score
Region growing [12]	0.68	0.69	0.35	0.63	0.44
Splitting/merging [51]	0.81	**0.99**	**0.81**	0.08	0.14
Global thresholding [21]	0.79	0.81	0.52	0.69	0.56
Niblack method [34]	0.81	0.81	0.51	**0.82**	**0.61**
Fuzzy C-means [30]	**0.82**	0.91	0.61	0.45	0.49
Canny [35]	0.79	0.96	0.45	0.11	0.17
Sobel [35]	0.80	0.99	0.66	0.03	0.06
Active contours without edges [13]	0.80	0.85	0.51	0.57	0.52
Level set method [5]	0.76	0.78	0.48	0.68	0.52
Watershed [14]	0.77	0.75	0.48	0.82	0.58
Mask R-CNN	**0.98**	**0.99**	**0.94**	**0.84**	**0.88**

to the splitting/merging one, considering the other metrics, Mask R-CNN are clearly superior. Also, it is noteworthy that there is no any other unsupervised method presenting all the metrics consistently high as the deep learning approach does.

B. Qualitative analysis

Figure 5 depicts a mosaic with the best results, while Figure 6 illustrates the worst results, in each metric. The image mosaics are comprised by the original X-ray images, ground truth, tooth segmentation and instance segmentation of each tooth, from left to right columns, respectively. The best segmentations (see Fig. 5) are achieved through near perfect results, except the recall and the F1-score, which ultimately demands a very balanced result between recall and precision (harmonic mean) to be high. In the worst segmentation examples (see Fig. 6), even the accuracy and specificity achieved high values; however, F1-score, precision and recall presented very poor results. After a visual analysis, this result was expected because of the artifacts not learned in the training process. This is the case 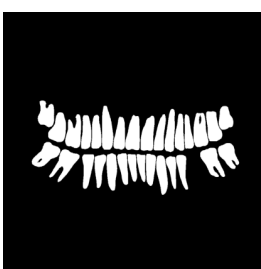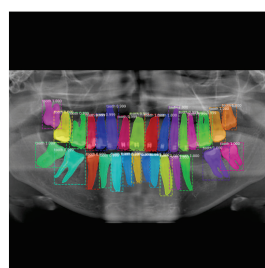of the images in the rows two, three and four (top-down view) in Fig. 6: Note that panoramic X-ray images two and four are the same ones, where the two metrics, F1-score and recall, achieved poor results, while in row three, we can see a prosthesis being considered as a tooth, while just one tooth was detected by Mask R-CNN (that is the reason of 48% of precision). Very low standard deviation (see Table II) indicates that bad segmentation could rarely be perceived.

IV. CONCLUSION

Segmenting teeth in dental X-ray images has been pursuit for many years, mainly relying in unsupervised methods. Although many approaches were proposed and tested, successful results were still far from being reached. Segmenting tooth in buccal images are mandatory for more complex tasks in decision support systems. This is the first step to detect not only teeth and their constituent parts, but also artifacts (*e.g.*, prosthesis), tooth problems, and even missing teeth. Considering that our proposed deep learning system demonstrated promising results on a challenging data set, future work resides on the instance segmentation of each component part of the mouth and teeth, as well as detection of missing teeth, all these with the goal of automatically generating medical reports.

REFERENCES

[1] Y. Y. Amer and M. J. Aqel, "An efficient segmentation algorithm for panoramic dental images," *Procedia Computer Science*, vol. 65, pp. 718–725, 2015.

[2] C. W. Wang, C. T. Huang, J. H. Lee, C. H. Li, S. W. Chang, M. J. Siao, T. M. Lai, B. Ibragimov, T. Vrtovec, O. Ronneberger, P. Fischer, T. F. Cootes, and C. Lindner, "A benchmark for comparison of dental radiography analysis algorithms," *Medical Image Analysis*, vol. 31, pp. 63–76, 2016.

[3] G. Silva, L. Oliveira, and M. Pithon, "Automatic segmenting teeth in x-ray images: Trends, a novel data set, benchmarking and future perspectives," *Expert Systems with Applications*, vol. 107, pp. 15 – 31, 2018.

[4] A. K. Jain and H. Chen, "Matching of dental x-ray images for human identification," *Pattern Recognition*, vol. 37, no. 7, pp. 1519–1532, 2004.

[5] A. Ehsani Rad, M. S. Mohd Rahim, and A. Norouzi, "Digital Dental X-Ray Image Segmentation and Feature Extraction," *TELKOMNIKA Indonesian Journal of Electrical Engineering*, vol. 11, no. 6, pp. 3109–3114, 2013.

[6] N. Senthilkumaran, "Genetic Algorithm Approach to Edge Detection for Dental X-ray Image Segmentation," *International Journal of Advanced Research in Computer Science and Electronics Engineering*, vol. 1, no. 7, pp. 5236–5238, 2012.

[7] O. Nomir and M. Abdel-Mottaleb, "Fusion of matching algorithms for human identification using dental x-ray radiographs," *IEEE Transactions on Information Forensics and Security*, vol. 3, no. 2, pp. 223–233, 2008.

[8] P. L. Lin, Y. H. Lai, and P. W. Huang, "An effective classification and numbering system for dental bitewing radiographs using teeth region and contour information," *Pattern Recognition*, vol. 43, no. 4, pp. 1380–1392, 2010.

[9] P. L. Lin and Y. H. Lai, "Dental biometrics: Human identification based on teeth and dental works in bitewing radiographs," *Pattern Recognition*, vol. 45, no. 3, pp. 934–946, 2012.

[10] F. Keshtkar and W. Gueaieb, "Segmentation of dental radiographs using a swarm intelligence approach," in *Canadian Conference on Electrical and Computer Engineering*, 2007, pp. 328–331.

[11] O. Nomir and M. Abdel-Mottaleb, "Hierarchical contour matching for dental X-ray radiographs," *Pattern Recognition*, vol. 41, no. 1, pp. 130–138, 2008.

[12] C. K. Modi and N. P. Desai, "A simple and novel algorithm for automatic selection of ROI for dental radiograph segmentation," in *Canadian Conference on Electrical and Computer Engineering*, 2011, pp. 000 504–000 507.

[13] R. B. Ali, R. Ejbali, and M. Zaied, "GPU-based Segmentation of Dental X-ray Images using Active Contours Without Edges," in *International Conference on Intelligent Systems Design and Applications*, vol. 1, 2015, pp. 505–510.

[14] H. Li, G. Sun, H. Sun, and W. Liu, "Watershed algorithm based on morphology for dental x-ray images segmentation," in *International Conference on Signal Processing Proceedings*, vol. 2, 2012, pp. 877–880.

[15] J. Kaur and J. Kaur, "Dental image disease analysis using pso and backpropagation neural network classifier," *International Journal of*

Advanced Research in Computer Science and Software Engineering, vol. 6, no. 4, pp. 158–160, 2016.

[16] R. Cameriere, S. De Luca, N. Egidi, M. Bacaloni, P. Maponi, L. Ferrante, and M. Cingolani, "Automatic age estimation in adults by analysis of canine pulp/tooth ratio: Preliminary results," *Journal of Forensic Radiology and Imaging*, vol. 3, no. 1, pp. 61–66, 2015.

[17] P. L. Lin, P. Y. Huang, P. W. Huang, H. C. Hsu, and C. C. Chen, "Teeth segmentation of dental periapical radiographs based on local singularity analysis," *Computer Methods and Programs in Biomedicine*, vol. 113, no. 2, pp. 433–445, 2014.

[18] S. Li, T. Fevens, A. Krzyzak, and S. Li, "An automatic variational level set segmentation framework for computer aided dental x-rays analysis in clinical environments," *Computerized Medical Imaging and Graphics*, vol. 30, no. 2, pp. 65–74, 2006.

[19] S. Dighe and S. Revati, "Preprocessing, Segmentation and Matching of Dental Radiographs used in Dental Biometrics," *International Journal of Science and Applied Information Technology*, vol. 1, no. 2278, pp. 52–56, 2012.

[20] S. Li, T. Fevens, A. Krzyzak, C. Jin, and S. Li, "Semi-automatic computer aided lesion detection in dental x-rays using variational level set," *Pattern Recognition*, vol. 40, no. 10, pp. 2861–2873, 2007.

[21] C. H. Huang and C. Y. Hsu, "Computer-assisted orientation of dental periapical radiographs to the occlusal plane," *Oral Surgery, Oral Medicine, Oral Pathology, Oral Radiology and Endodontology*, vol. 105, no. 5, pp. 649–653, 2008.

[22] P. L. Lin, P. W. Huang, P. Y. Huang, and H. C. Hsu, "Alveolar bone-loss area localization in periodontitis radiographs based on threshold segmentation with a hybrid feature fused of intensity and the h-value of fractional brownian motion model," *Computer Methods and Programs in Biomedicine*, vol. 121, no. 3, pp. 117–126, 2015.

[23] D. Bruellmann, S. Sander, and I. Schmidtmann, "The design of an fast Fourier filter for enhancing diagnostically relevant structures - endodontic files," *Computers in Biology and Medicine*, vol. 72, pp. 212–217, 2016.

[24] P. L. Lin, P. Y. Huang, and P. W. Huang, "An effective teeth segmentation method for dental periapical radiographs based on local singularity," in *IEEE International Conference on System Science and Engineering*, vol. 1, 2013, pp. 407–411.

[25] U. A. A. Niroshika, R. G. N. Meegama, and T. G. I. Fernando, "Active contour model to extract boundaries of teeth in dental X-ray images," in *Proceedings of the 8th International Conference on Computer Science and Education, ICCSE 2013*, no. Iccse, 2013, pp. 396–401.

[26] S. Tikhe, A. Naik, S. Bhide, T. Saravanan, and K. Kaliyamurthie, "Algorithm to Identify Enamel Caries and Interproximal Caries Using Dental Digital Radiographs," in *International Advanced Computing Conference, IACC 2016*, 2016, pp. 225–228.

[27] N. Senthilkumaran, "Fuzzy Logic Approach to Edge Detection for Dental X-ray Image Segmentation," *International Journal of Computer Science and Information Technologies*, vol. 3, no. 5, pp. 5236–5238, 2012.

[28] P.-l. An, P. Huang, P. Whe, H. U. Ang, C. Science, I. Engineering, and C. Science, "An automatic lesion detection method for dental x-ray images by segmentation using variational level set," in *Proceedings of the 2012 International Conference on Machine Learning and Cybernetics, Xian*, vol. 1, 2012, pp. 1821–1825.

[29] T. Economopoulos, G. K. Matsopoulos, P. A. Asvestas, K. Gröndahl, and H. G. Gröndahl, "Automatic correspondence using the enhanced hexagonal centre-based inner search algorithm for point-based dental image registration," *Dentomaxillofacial Radiology*, vol. 37, no. 4, pp. 185–204, 2008.

[30] M. K. Alsmadi, "A hybrid fuzzy c-means and neutrosophic for jaw lesions segmentation," *Ain Shams Engineering Journal*, 2015.

[31] A. Lurie, G. M. Tosoni, J. Tsimikas, and W. Fitz, "Recursive hierarchic segmentation analysis of bone mineral density changes on digital panoramic images," *Oral Surgery, Oral Medicine, Oral Pathology and Oral Radiology*, vol. 113, no. 4, pp. 549–558, 2012.

[32] A. Ajaz and D. Kathirvelu, "Dental biometrics: Computer aided human identification system using the dental panoramic radiographs," in *International Conference on Communication and Signal Processing*, 2013, pp. 717–721.

[33] R. Indraswari, A. Z. Arifin, D. A. Navastara, and N. Jawas, "Teeth segmentation on dental panoramic radiographs using decimation-free directional filter banck thresholding and multistage adaptive threshold-

ing," in *International Conference on Information and Communication Technology and System*, vol. 1, 2015, pp. 49–54.

[34] M. R. Mohamed Razali, N. S. Ahmad, Z. Mohd Zaki, and W. Ismail, "Region of adaptive threshold segmentation between mean, median and otsu threshold for dental age assessment," in *International Conference on Computer, Communications, and Control Technology*, no. I4ct, 2014, pp. 353–356.

[35] M. R. M. Razali, N. S. Ahmad, R. Hassan, Z. M. Zaki, and W. Ismail, "Sobel and canny edges segmentations for the dental age assessment," in *Intl. Conference on Computer Assisted System in Health*, 2015, pp. 62–66.

[36] M. M. Hasan, R. Hassan, and W. Ismail, "Automatic segmentation of jaw from panoramic dental x-ray images using gvf snakes," in *WAC*, vol. 1, 2016, pp. 1–6.

[37] L. Gráfová, M. Kašparová, S. Kakawand, A. Procházka, and T. Dostálová, "Study of edge detection task in dental panoramic radiographs," *Dentomaxillofacial Radiology*, vol. 42, no. 7, 2013.

[38] E. Said, D. Nassar, G. Fahmy, and H. Ammar, "Teeth segmentation in digitized dental x-ray films using mathematical morphology," *IEEE Transactions on Information Forensics and Security*, vol. 1, no. 2, pp. 178–189, 2006.

[39] L. H. Son and T. M. Tuan, "A cooperative semi-supervised fuzzy clustering framework for dental X-ray image segmentation," *Expert Systems with Applications*, vol. 46, pp. 380–393, 2016.

[40] W. G. M. Geraets, J. G. C. Verheij, P. F. van der Stelt, K. Horner, C. Lindh, K. Nicopoulou-Karayianni, R. Jacobs, E. J. Harrison, J. E. Adams, and H. Devlin, "Prediction of bone mineral density with dental radiographs," *Bone*, vol. 40, no. 5, pp. 1217–1221, 2007.

[41] D. N. Trivedi, A. M. Kothari, S. Shah, and S. Nikunj, "Dental Image Matching By Canny Algorithm for Human Identification," *International Journal of Advanced Computer Research*, vol. 4, no. 17, pp. 985–990, 2015.

[42] O. Ronneberger, P. Fischer, and T. Brox, "U-Net: Convolutional Networks for Biomedical Image Segmentation," pp. 1–8, 2015.

[43] "Locality Sensitive Deep Learning for Detection and Classification of Nuclei in Routine Colon Cancer Histology Images," *IEEE Transactions on Medical Imaging*, vol. 35, no. 5, pp. 1196–1206, 2016.

[44] B. Ait Skourt, A. El Hassani, and A. Majda, "Lung CT Image Segmentation Using Deep Neural Networks," *Procedia Computer Science*, vol. 127, pp. 109–113, 2018.

[45] W. Dai, J. Doyle, X. Liang, H. Zhang, N. Dong, Y. Li, and E. P. Xing, "SCAN: Structure Correcting Adversarial Network for Organ Segmentation in Chest X-rays," 2017.

[46] T. Lin, M. Maire, S. J. Belongie, L. D. Bourdev, R. B. Girshick, J. Hays, P. Perona, D. Ramanan, P. Dollár, and C. L. Zitnick, "Microsoft COCO: common objects in context," *CoRR*, vol. abs/1405.0312, 2014. [Online]. Available: http://arxiv.org/abs/1405.0312

[47] K. He, G. Gkioxari, P. Dollár, and R. B. Girshick, "Mask R-CNN," *CoRR*, vol. abs/1703.06870, 2017. [Online]. Available: http://arxiv.org/abs/1703.06870

[48] S. Ren, K. He, R. Girshick, and J. Sun, "Faster r-cnn: Towards real-time object detection with region proposal networks," in *Advances in neural information processing systems*, 2015, pp. 91–99.

[49] J. Long, E. Shelhamer, and T. Darrell, "Fully convolutional networks for semantic segmentation," in *IEEE Conf. on Comp. Vision and Pattern Recog.*, 2015, pp. 3431–3440.

[50] D. P. Kingma and J. L. Ba, "Adam: A method for stochastic optimization," in *Proc. 3rd Int. Conf. Learn. Representations*, 2014.

[51] R. B. Subramanyam, K. P. Prasad, and B. Anuradha, "Different image segmentation techniques for dental image extraction," *Int. J. Eng. Res. Appl*, vol. 4, no. 7, pp. 173–177, 2014.